

(2006) 5(4), 916-924 doi: 10.1021/pr-0504079

## Proteomic Analysis of the Mode of Antibacterial Action of Silver Nanoparticles

Chun-Nam Lok,<sup>†,§,||</sup> Chi-Ming Ho,<sup>†,‡</sup> Rong Chen,<sup>†,‡</sup> Qing-Yu He,<sup>†,‡</sup> Wing-Yiu Yu,<sup>†,‡</sup>  
Hongzhe Sun,<sup>†,‡</sup> Paul Kwong-Hang Tam,<sup>†,‡</sup> Jen-Fu Chiu,<sup>\*,†,§,||</sup> and Chi-Ming Che<sup>\*,†,‡</sup>

Open Laboratory of Chemical Biology of the Institute of Molecular Technology for Drug Discovery and Synthesis, Department of Chemistry, Institute of Molecular Biology, Department of Anatomy, Department of Surgery, and Genome Research Centre, The University of Hong Kong, Pokfulam, Hong Kong, China

Silver nanoparticles (nano-Ag) are potent and broad-spectrum antimicrobial agents. In this study, spherical nano-Ag (average diameter = 9.3 nm) particles were synthesized using a borohydride reduction method and the mode of their antibacterial action against *E. coli* was investigated by proteomic approaches (2-DE and MS identification), conducted in parallel to analyses involving solutions of Ag<sup>+</sup> ions. The proteomic data revealed that a short exposure of *E. coli* cells to antibacterial concentrations of nano-Ag resulted in an accumulation of envelope protein precursors, indicative of the dissipation of proton motive force. Consistent with these proteomic findings, nano-Ag were shown to destabilize the outer membrane, collapse the plasma membrane potential and deplete the levels of intracellular ATP. The mode of action of nano-Ag was also found to be similar to that of Ag<sup>+</sup> ions (e.g., Dibrov, P. et al, *Antimicrob. Agents Chemother.* **2002**, 46, 2668–2670); however, the effective concentrations of nano-Ag and Ag<sup>+</sup> ions were at nanomolar and micromolar levels, respectively. Nano-Ag appear to be an efficient physicochemical system conferring antimicrobial silver activities.

**Keywords:** silver nanoparticles • silver ions • antibacterial agents • *E. coli* • outer membrane proteins • membrane potential • ATP

### Introduction

It has been known since ancient times that silver and its compounds are effective antimicrobial agents.<sup>1–3</sup> Legendary examples include the use of diluted solution of silver salts in the prophylactic treatment of newborn eye infections and in the treatment of burn wounds. Currently, silver-containing agents are regularly used in clinical wound dressings (e.g., silver sulfadiazine) as well as in the coatings of biomedical materials (e.g., silver impregnated catheters).

A number of chemical forms of silver are known to exhibit antimicrobial activities. Ag<sup>+</sup> ions in the form of a silver nitrate solution is the prototypical antimicrobial silver species. The biocidal effect of Ag<sup>+</sup>, with its broad spectrum of activity including bacterial, fungal, and viral agents, can be achieved at submicromolar concentrations.<sup>1</sup> In addition, tarnished bulk

silver has also been reported to be antimicrobial, ascribed to its surface oxide layer and/or release of Ag (I) species.<sup>1,4</sup> Novel composite materials for the delivery of biocidal Ag<sup>+</sup> ions are continuously being developed.<sup>5</sup>

Another antimicrobial silver species that has been known for a long time, but has received little attention, is the nanometer-sized silver particles (silver nanoparticles, nano-Ag).<sup>6</sup> However, the recent advances in research on metal nanoparticles appears to revive the use of nano-Ag in various biomedical applications. nano-Ag prepared by a variety of synthetic methods have been shown to be effective antimicrobial agents.<sup>7–11</sup> For example, wound dressings based on sputtered nano-Ag are employed in clinical practice to suppress microbial infection in burn wounds.<sup>12</sup> Recently, our group also demonstrated that nano-Ag synthesized by borohydride reduction exhibit cytoprotective activities toward human immunodeficiency virus-1 infected cells.<sup>13</sup>

The antimicrobial modes of action of Ag<sup>+</sup> ions have been known in some details. Micromolar levels of Ag<sup>+</sup> ions have been reported to uncouple respiratory electron transport from oxidative phosphorylation,<sup>14,15</sup> inhibit respiratory chain enzymes,<sup>15–17</sup> or interfere with the membrane permeability to protons and phosphate.<sup>15,18</sup> In addition, higher concentrations of Ag<sup>+</sup> ions have been shown to interact with cytoplasmic components and nucleic acids.<sup>19,20</sup> As for nano-Ag, recent electron microscopic studies have revealed that the majority of nano-Ag were localized in the membranes of treated *E. coli*

\* To whom correspondence should be addressed. Chi-Ming Che, Department of Chemistry, The University of Hong Kong, Pokfulam Road, Hong Kong. Tel: 852-2859-2154. Fax: 852-2857-1586. E-mail: cmche@hku.hk. Jen-Fu Chiu, 8N-12, Kadoorie Biological Sciences Building, The University of Hong Kong, Pokfulam Road, Hong Kong. Tel: 852-2299-0777. Fax: 852-2817-1006. E-mail: jfchiu@hkucc.hku.hk.

<sup>†</sup> Open Laboratory of Chemical Biology of the Institute of Molecular Technology for Drug Discovery and Synthesis.

<sup>‡</sup> Department of Chemistry, The University of Hong Kong.

<sup>§</sup> Institute of Molecular Biology, The University of Hong Kong.

<sup>||</sup> Department of Anatomy, The University of Hong Kong.

<sup>||</sup> Department of Surgery, The University of Hong Kong.

<sup>#</sup> Genome Research Centre, The University of Hong Kong.



cells, while some penetrated into the cells.<sup>10</sup> However, the biochemical and molecular aspects of the actions of this distinct silver species have never been directly addressed.

In this study, we employed a proteomic approach (two-dimensional electrophoresis and proteins identification by mass spectrometry) to investigate the mode of antibacterial action of nano-Ag against *E. coli*, with parallel analyses conducted with solutions of Ag<sup>+</sup> ions. Together with supporting biochemical studies, our results reveal, for the first time, several primary actions of nano-Ag in *E. coli* cells, namely in envelope protein processing, outer membrane permeability, plasma membrane potential and energization

## Materials and Methods

**Synthesis of Nano-Ag.** Nano-Ag particles were synthesized by the borohydride reduction of AgNO<sub>3</sub> in the presence of citrate as a stabilizing agent as previously described.<sup>21</sup> Briefly, NaBH<sub>4</sub> (50 mg) was added to a vigorously stirred AgNO<sub>3</sub> solution (16 mg in 1 L) and sodium citrate (0.7 mM) at room temperature. A golden yellow solution was formed, showing a surface plasmon resonance (SPR) absorption peak at ~400 nm. The solution was concentrated further to 100 mL under vacuum. Nanoparticles were examined using Philips Tecnai 20 transmission electron microscope (TEM) equipped with energy dispersive analysis of X-ray. TEM micrographs revealed that nano-Ag were spherical with diameter of  $9.3 \pm 2.8$  nm (Figure 1A), based on the measurement of 300 particles measurement at five sites selected at random.

Determination of the particle concentration of nano-Ag preparations were based on calculations using silver density (10.5 g/cm<sup>3</sup> at 300K). The particle concentrations in the stock was ~40 nM, corresponding to 108 µg Ag/mL. The concentrations of nano-Ag indicated in this paper are quoted as the number of moles of nanoparticles per unit volume in nM.

To show that it was the nano-Ag in our preparations were the principal antibacterial agent, nano-Ag diluted in assay medium (Hepes buffer and M9 medium) were passed through a centricon membrane with a molecular weight cut off at 3 kDa (YM-3, Millipore). The filtrates obtained, which contained about 0.1% of the total silver loaded as determined by inductive coupled plasma-mass spectrometry (ICP-MS, Agilent, 7500), did not exhibit antibacterial activity. There was no loss of antibacterial activities in the retained concentrates, which mainly contained the nanoparticles.

**Bacterial Culture and Sample Preparation for 2-DE.** *E. coli* cells (wild-type K12 strain, MG1655) were obtained from the *E. coli* Genetic Stock Center, Yale University. *E. coli* cells were grown at 35 °C with shaking to early exponential phase (O. D.<sub>650</sub> = 0.15) in M9 defined medium (47 mM Na<sub>2</sub>HPO<sub>4</sub>, 22 mM KH<sub>2</sub>PO<sub>4</sub>, 8.6 mM NaCl, 18 mM NH<sub>4</sub>Cl, 2 mM MgCl<sub>2</sub>, 0.1 mM CaCl<sub>2</sub>, supplemented with 0.4% glucose). Nano-Ag are known to aggregate in medium of high salt content<sup>22</sup> and lose their antibacterial activities. To stabilize the nanoparticles, bovine serum albumin (BSA) was premixed with nano-Ag before adding to the medium (0.1% final).<sup>13,22</sup> The antibacterial concentrations of nano-Ag or AgNO<sub>3</sub> were determined by monitoring the O. D.<sub>650</sub> of the bacterial culture turbidity. For sample preparation for 2-DE, 20 mL of the growing bacteria culture (O. D.<sub>650</sub> = 0.15) were treated with antibacterial concentrations of nano-Ag or AgNO<sub>3</sub> for 30 min. Cells were collected by centrifugation and suspended in lysis buffer (8 M urea, 4% CHAPS, 20 mM dithiothreitol). The lysates were

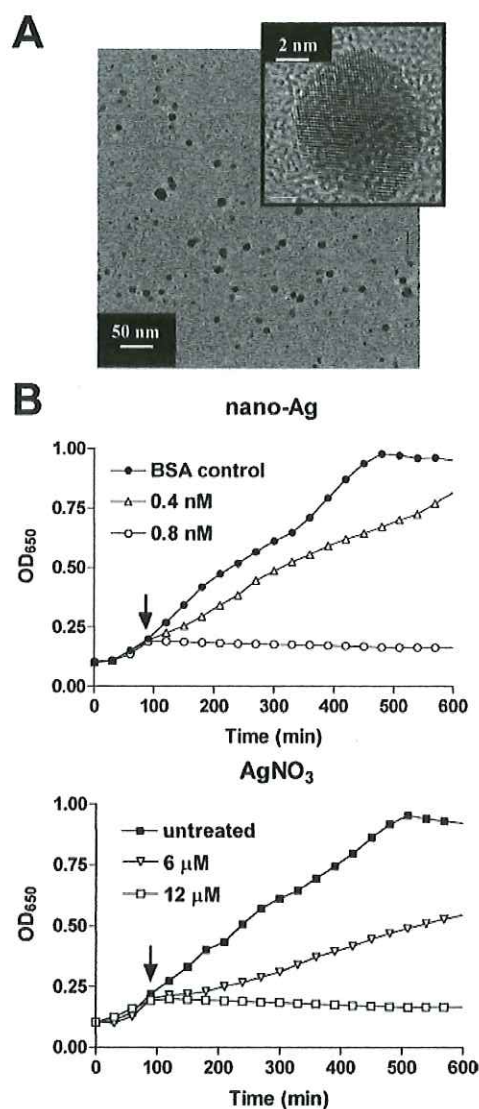


**Figure 1.** (A) Images of transmission electron microscopy (TEM) and high-resolution transmission electron microscopy (HRTEM, insert) of nano-Ag prepared using the borohydride reduction method. (B) Antibacterial activities of nano-Ag and AgNO<sub>3</sub>. *E. coli* cells were grown at 35 °C to the early exponential phase (O. D.<sub>650</sub> = 0.15) in M9 defined medium. Nano-Ag (0.4 and 0.8 nM, stabilized with BSA) or AgNO<sub>3</sub> (6 and 12 µM) was added at the time indicated by the arrows and the O. D.<sub>650</sub> was monitored continuously.

clarified by centrifugation and the supernatants were stored at -80 °C before analysis by 2-DE.

**2-DE.** 2-DE was performed with the IPGphor IEF and electrophoresis system (GE Health Care). Protein lysates (50 µg of total proteins) were mixed with rehydration solution containing 8 M urea, 4% CHAPS, 20 mM dithiothreitol to obtain a final volume of 250 µL and IPG buffer was added to 0.5%. The rehydration step was carried out with IPG strips (13 cm, pH range 4–7) for 10 h at 30 V. IEF conditions were: 500 and 1000 V for 1 h each and 8000 V for 10 h with a total of 56 KVh. After IEF, the strips were incubated for 15 min in equilibration buffer (6 M urea, 30% glycerol, 2% SDS, 50 mM Tris-HCl, pH 6.8) containing 1% dithiothreitol (w/v), and then another 15 min with equilibration buffer containing 2.5% w/v iodoacetamide. For second-dimension SDS-PAGE, the strips were

transferred onto 12.5% polyacrylamide slab gels containing 0.1% SDS and electrophoresed. All gels were visualized by silver staining and scanned with ImageScanner (GE Health Care). Protein spots on the image files were detected and quantified using ImageMaster 2D Elite software (GE Health Care). Experiments were performed twice and protein spots exhibiting consistent differences between samples were excised from the gels. After in-gel tryptic digestion, the resulting peptides were identified by MALDI-TOF MS.

**MALDI-TOF MS and MS/MS.** MS spectra were recorded at the Genome Research Centre or the Department of Chemistry, the University of Hong Kong, using a MALDI-TOF mass spectrometer (Voyager-DE STR, Applied Biosystems). Full scan mass spectra from 800 to 2500  $m/z$  were collected in the reflection mode with an acceleration voltage of 20 kV. At least 100 MS spectra were accumulated for data processing. NCBI database searching was performed manually using the Mascot (<http://www.matrixscience.com>) or MS-Fit programs (<http://prospector.ucsf.edu>) with a mass tolerance setting of 50 ppm.

Peptides of interest were further analyzed by MS/MS on a hybrid quadrupole-time-of-flight mass spectrometer (QSTAR-XL, Applied Biosystems), equipped with a MALDI source and laser ( $N_2$ , 337 nm, 20 Hz) with an energy adjustable collision cell filled with pure argon. Experimental fragment masses were used to search the NCBI database for protein identifications using the Mascot program. Peptides with a minimum of four consecutive b- and y-ions were considered as an acceptable match.

**Immunoblots.** For 1D immunoblots, 10  $\mu$ g of protein lysates were mixed with SDS loading buffer (40 mM Tris HCl, pH 6.8, 2% SDS, 20 mM dithiothreitol, 10% glycerol, 0.1% bromophenol blue), heated at 70°C for 3 min and electrophoresed on a 12.5% polyacrylamide gel containing 0.1% SDS. The proteins on the gel were then transferred to PVDF membranes by semidry blotting units (GE Health Care). For 2D-immunoblots, proteins on the 2D gels were transferred in the same manner. The blots were blocked with 4% skim milk in Tris-buffered saline supplemented with 0.1% Tween 20. OmpA proteins were detected with polyclonal rabbit antibodies raised against *E. coli* OmpA (obtained from Prof. Arnold Driessen, University of Groningen, Netherlands) followed by horseradish peroxidase conjugated goat anti-rabbit IgG antibodies. Immunoreactivities were visualized by ECL chemiluminescence detection (GE Health Care).

**Outer Membrane Destabilization Assays.** The effects of nano-Ag or  $AgNO_3$  on the outer membrane were studied by examining their sensitization to detergent mediated bacteriolysis.<sup>23</sup> Exponentially growing *E. coli* cells were suspended to an O. D.<sub>650</sub> of 0.1 in 50 mM sodium Hepes buffer (pH 7.0) containing 5 mM glucose, and then treated with nano-Ag or  $AgNO_3$  at room temperature for 5 min. The mixtures were centrifuged and the medium was removed. The cell pellets were resuspended in the same volume of assay buffer without silver, then SDS (0.1% final concentration) was added and the O. D.<sub>650</sub> was continuously monitored.

**Membrane Potential Assays.** Membrane potential assays were performed according to the established procedures using the membrane potential probe 3,5-dipropylthiadicarbocyanine iodide (diSC<sub>3</sub>(5), Molecular Probes).<sup>24–26</sup> To allow uptake of diSC<sub>3</sub>(5), exponentially growing *E. coli* cells were first washed with 0.1 M Tris HCl (pH 8.0), and resuspended in the same buffer to an O. D.<sub>650</sub> of 10. Then cells were treated with 1 mM EDTA for 90 s at 35 °C. After that, cells were washed and added

to a buffer containing 50 mM potassium Hepes (pH 7.0), 5 mM glucose and 0.2  $\mu$ M diSC<sub>3</sub>(5) to an O. D.<sub>650</sub> of 0.1. After stabilization of the fluorescence signals, nano-Ag or  $AgNO_3$  was added. The fluorescence was recorded with excitation at 620 nm and emission at 670 nm using Hitachi fluorescence spectrophotometer F-4500.

**Determination of Cellular Potassium Content.** *E. coli* cells were resuspended in 50 mM sodium Hepes buffer (pH 7.0) containing 5 mM glucose to an OD<sub>650</sub> of 0.1. After treatment with nano-Ag or  $AgNO_3$  treatment, cells were washed and the cell pellets were digested with nitric acid. The potassium contents were determined by flame atomic emission spectroscopy (FAES) (Perkin-Elmer, 3110).

**ATP Assays.** Exponentially growing *E. coli* cells were resuspended in 50 mM sodium Hepes buffer (pH 7.0) containing 5 mM glucose to an O. D.<sub>650</sub> of 0.1, and treated with nano-Ag or  $AgNO_3$  at room temperature. To determine the total ATP levels in the bacteria culture, aliquots were withdrawn and the ATP was extracted with 1% trichloroacetic acid in the presence of 2 mM EDTA. After incubation on ice for 30 min, the samples were neutralized with 2 volumes of 0.1 M Tris acetate (pH 7.8). Extracellular ATP levels were determined for the supernatants after centrifugation of the bacterial culture. ATP levels of the samples were determined by a luciferase-luciferin enzymatic assay kit from Molecular Probes.

**Bacteria Colony Counting Assays.** Minimum inhibitory concentration (MIC) of nano-Ag or  $AgNO_3$  was used in the outer membrane destabilization, membrane potential, and ATP assays. The MIC was defined as the lowest concentration that inhibited bacterial colony formation by 2 orders of magnitude after a 5-min incubation. Exponentially growing *E. coli* cells were suspended in 50 mM sodium Hepes buffer (pH 7.0) containing 5 mM glucose to an O. D.<sub>650</sub> of 0.1. After treatment with nano-Ag or  $AgNO_3$ , aliquots were taken, diluted appropriately and spread on LB agar plates. Colonies were counted after incubation overnight at 37 °C. The use of Hepes buffer in the colony counting, outer membrane destabilization, membrane potential and ATP assays enabled stable dispersion of nano-Ag,<sup>13</sup> and consequently no BSA was added in these assays.

## Results

**Determination of Antibacterial Activities of Nano-Ag for Proteomic Analysis.** For the proteomic analyses, *E. coli* cells were grown in M9 culture medium to the exponential phase for optimal levels of growth and protein metabolism. The antibacterial activities of nano-Ag or  $AgNO_3$  against the growth of *E. coli* cells in M9 medium are shown in Figure 1B. Both silver species were found to elicit an immediate and sustained inhibition of *E. coli* cell proliferation. The concentrations of nano-Ag and  $AgNO_3$  at which the inhibition of bacterial proliferation became apparent were 0.4 nM and 6  $\mu$ M, respectively.

**Proteomic Analysis of *E. coli* Cells Treated with Nano-Ag.** Exponentially growing *E. coli* cells cultured in M9 medium were treated with antibacterial concentrations of nano-Ag (0.4 and 0.8 nM) or  $AgNO_3$  (6 and 12  $\mu$ M) for 30 min. The proteomes were then analyzed by 2-DE followed by silver staining. Representative 2D gel images are shown in Figure 2A. There was no dramatic global changes between the proteomes of the nano-Ag treated and untreated cells. However, the expressions of at least eight proteins were specifically stimulated in the

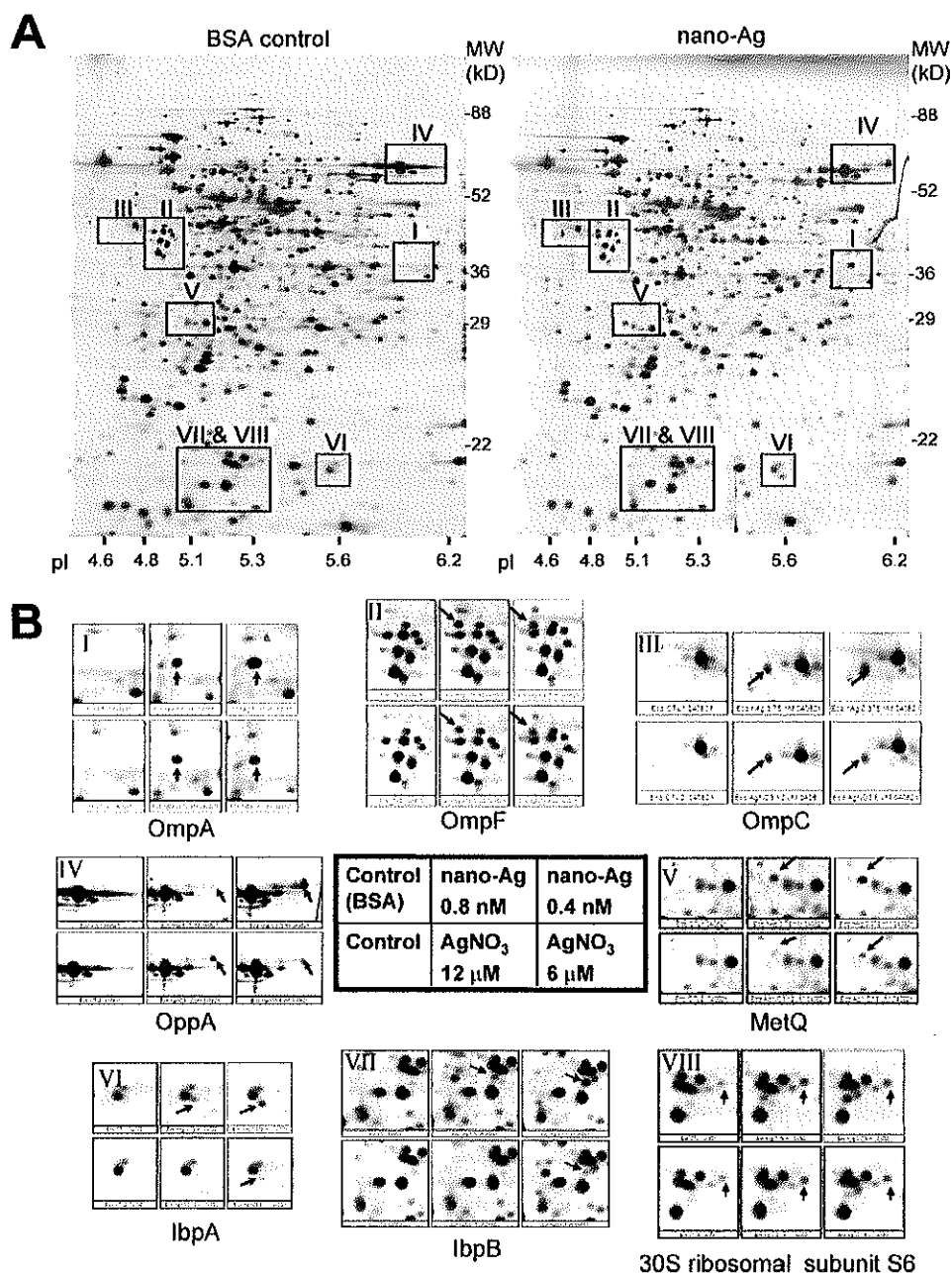


**Figure 2.** 2-DE analysis of protein samples from *E. coli* cells treated with nano-Ag or AgNO<sub>3</sub>. *E. coli* cells were grown at 35 °C to the early exponential phase (O. D.<sub>650</sub> = 0.15) in M9 medium, treated with nano-Ag (0.4 and 0.8 nM, with 0.1% BSA) or AgNO<sub>3</sub> (6 and 12 μM) for 30 min, then subjected to 2-DE analysis. (A) 2D gel images of *E. coli* cells treated with nano-Ag or BSA as a control. Squared areas (I–VIII) represent areas of interest containing the silver induced protein spots and are enlarged in (B).

nano-Ag treated cells (Figure 2B). Similar protein expression profiles were also found in *E. coli* cells treated with AgNO<sub>3</sub>.

The identification of proteins whose expressions were stimulated by nano-Ag was performed using MALDI-TOF MS and MS/MS on the tryptic digests of the protein spots of interest, with the results summarized in Table 1. These proteins include the outer membrane proteins A, C, and F (OmpA, OmpC and OmpF), periplasmic oligopeptide binding protein A (OppA), D-methionine binding lipoprotein (MetQ), inclusion body binding proteins A and B (IbpA and IbpB), and 30S ribosomal subunit S6. The essence of our proteomic data is that the expressions of a number of the cell envelope proteins (OmpA,

OmpC, OmpF, OppA and MetQ) were apparently stimulated by nano-Ag treatment. Upon closer inspection, the observed pI and Mr values of these stimulated proteins were consistent with those of their precursor forms, which generally contain a positively charged N-terminal signal sequence of around 2 kDa (Table 2). For example, the outer membrane protein A (OmpA) identified in the present study has a Mr of 37 kDa and pI of 6 that are consistent with the theoretical values of the full length OmpA precursor (proOmpA), but deviate from the calculated as well as documented values of the matured form (Mr = 35 kDa and pI = 5.5) (SWISS-2DPAGE database, <http://ca.expasy.org/ch2d> and references therein).

**Table 1.** List of Identified *E. coli* Proteins Whose Expressions Were Stimulated by Nano-Ag (>1.8 fold)

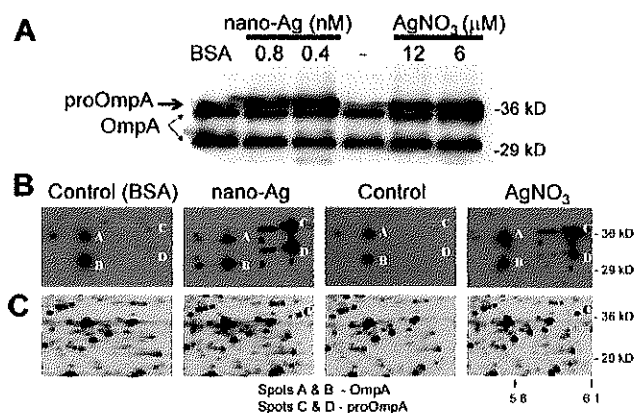
protein no.	protein description	accession no.	no. of peptides matched <sup>a</sup>	observed migration	
				<i>M<sub>r</sub></i> (kDa)	<i>pI</i>
I	Outer Membrane Protein A precursor (OmpA)	P02934	10	37	6.0
II	Outer Membrane Protein C precursor (OmpC)	P06996	12	40	4.6
III	Outer Membrane Protein F precursor (OmpF)	P02931	12	40	4.8
IV	Periplasmic Oligopeptide binding protein precursor (OppA)	P23843	17	60	6.1
V	D-Methionine binding lipoprotein precursor (MetQ)	P28635	6	29	5.1
VI	Inclusion body binding protein A (IbpA)	P29209	9	16	5.6
VII	Inclusion body binding protein B (IbpB)	P29210	6	16	5.2
VIII	30S ribosomal subunit S6	P02358	10	15	5.3

<sup>a</sup> See Supporting Information (Table 1S–9S).

**Table 2.** Comparison between the Calculated (theoretical), Documented and Observed Values of Several *E. coli* Envelope Proteins Whose Expressions Were Stimulated by Nano-Ag

	<i>pI</i>				<i>M<sub>r</sub></i> (kDa)			
	calculated <sup>a</sup>		2D gel		calculated <sup>a</sup>		2D gel	
	mature	precursor	observed	documented <sup>a</sup>	mature	precursor	observed	documented <sup>a</sup>
OmpA	5.61	5.99	6.0	5.3–5.5	35.2	37.2	37	28–34
OmpF	4.64	4.76	4.8	4.6–4.7	37.1	39.3	40	36–37
OppA	5.85	6.05	6.1	5.4–5.9	58.3	60.9	60	54–57
MetQ	4.93	5.13	5.1	4.9	27.2	29.4	29	27

<sup>a</sup> From SWISS-2DPAGE database (<http://ca.expasy.org/ch2>) and references therein.

**Figure 3.** Immunoblot analysis of the OmpA expression in nano-Ag or AgNO<sub>3</sub> treated *E. coli* cells. (A) 1D-immunoblot. The positions of OmpA (mature forms) and proOmpA (precursor form) are indicated. (B) 2D-immunoblots. Spots A and B correspond to mature forms of OmpA, whereas spots C and D correspond to OmpA precursors (proOmpA). (C) 2D gel images corresponding to the 2D-immunoblots shown in (B).

**Immunoblots of OmpA.** The accumulation of precursor forms of the envelope proteins in the nano-Ag treated *E. coli* cells was further investigated. Attempts to identify the N-terminal signal sequences of the precursors in tryptic digests of the envelope proteins by MS were not successful, presumably due to insufficient peptide mass coverage. Instead, we examined the expression of OmpA by immunoblots in detail. Figure 3A shows that three protein bands were detected on the 1D immunoblot probed with polyclonal antibodies raised against the OmpA protein. The observed expression pattern was very similar to those reported previously:<sup>27–32</sup> mature OmpA appears in both heat-modified (35 kDa) and unmodified forms (30 kDa), whereas proOmpA appears in a higher molecular weight form (37 kDa) on SDS-PAGE. In nano-Ag treated cells, the expression of the 37 kDa band, corresponding to proOmpA, was markedly

enhanced. This is consistent with the stimulated expression of the OmpA spot (37 kDa) in nano-Ag treated cells, as shown on the 2D gels (Figure 2B).

2D immunoblots were also performed to further locate the OmpA precursors and its mature forms (Figure 3B). In both control and nano-Ag treated samples, two protein spots, A and B, of the same *pI* (5.6) but different *M<sub>r</sub>* (30 and 35 kDa) were identified. These two spots most probably correspond to the unmodified (30 kDa) and heat-modified forms of mature OmpA (35 kDa), which were also shown in the 1D immunoblot blot (Figure 3A). However, in nano-Ag treated cells, additional protein spots with *pI* = 5.7–6.0 were identified. Spot C (*pI* = 6, *M<sub>r</sub>* = 37 kDa) could be aligned with the nano-Ag induced OmpA spots appearing on the silver stained 2D gels (Figure 2, area I, and Figure 3C). Taking its *pI* (pH 6) and *M<sub>r</sub>* (37 kDa) into consideration, this spot most probably corresponds to the denatured form of proOmpA (Table 2). Another protein spot, D, had the same *pI* as proOmpA, but increased gel mobility. This presumably relates to a previously described partially denatured form of proOmpA, which appeared to have similar mobility.<sup>27</sup> A number of minor spots were also arranged in a close array between the precursor and mature forms, most likely corresponding to processing intermediates and/or post-translationally modified species. The expression of OmpA was found to be similarly altered in the AgNO<sub>3</sub> treated cells.

It is also noteworthy that the outer membrane protein precursors are known to have extremely short cellular half-lives (3–5 s),<sup>31</sup> and are not normally detected under normal conditions.<sup>27–33</sup> This was the case for the untreated samples in our experiments (Figure 2B and 3B). Thus, our proteomic analysis and immunoblot assays demonstrated that nano-Ag treatment resulted in an accumulation of precursor forms of OmpA, apparently due to an inhibition of their processing into shorter, mature forms.

**Effects of Nano-Ag on Membrane Properties of *E. coli*.** Observing an accumulation of envelope protein precursors in the nano-Ag treated cells provides clues to elucidate a possible

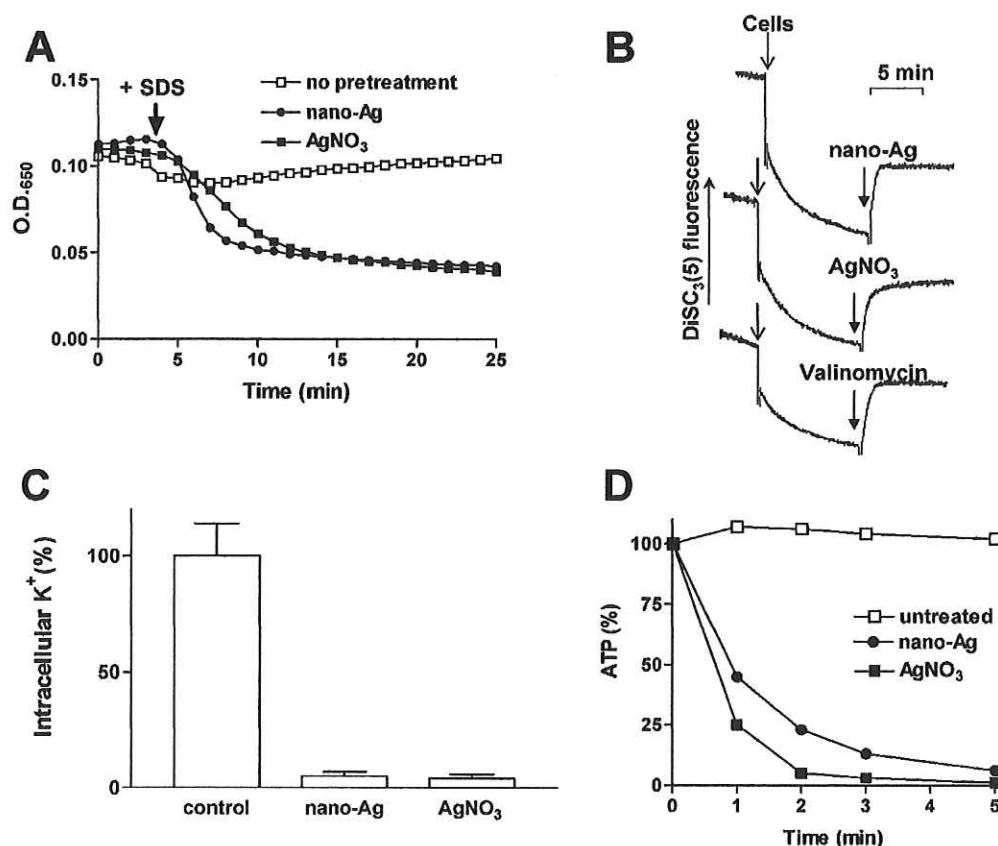


**Figure 4.** Effects of nano-Ag and AgNO<sub>3</sub> on *E. coli* membrane properties. (A) Outer membrane destabilization assays. Exponentially growing *E. coli* cells were resuspended to an O. D.<sub>650</sub> of 0.1 in 50 mM sodium Hepes buffer (pH 7.0) containing 5 mM glucose, and treated with nano-Ag (1 nM) or AgNO<sub>3</sub> (1  $\mu$ M) at room temperature for 5 min. Cells were then centrifuged and the cell pellets were resuspended in the same volume of assay buffer without silver. SDS (0.1% final) was then added and the degree of bacteriolysis was determined by measuring the O. D.<sub>650</sub>. (B) Membrane potential assays. Exponentially growing *E. coli* cells were treated with EDTA to facilitate uptake of the membrane potential probe, diSC<sub>3</sub>(5). Cells were resuspended to an O. D.<sub>650</sub> of 0.1 in a buffer containing 50 mM potassium Hepes (pH 7.0), 5 mM glucose and 0.2  $\mu$ M diSC<sub>3</sub>(5), before recording the fluorescence at room temperature. The fluorescence tracings of diSC<sub>3</sub>(5) are shown, with arrows indicating the addition of *E. coli* cells and nano-Ag (1 nM), AgNO<sub>3</sub> (1  $\mu$ M) or valinomycin (1  $\mu$ M). (C) Cellular potassium content. Exponentially growing *E. coli* cells were resuspended to an O. D.<sub>650</sub> of 0.1 in a buffer containing 50 mM sodium Hepes (pH 7.0) and 5 mM glucose, and treated with nano-Ag (1 nM) or AgNO<sub>3</sub> (1  $\mu$ M) at room temperature for 5 min. Cells were harvested, washed, and the cell-associated potassium content was determined by FAES. The potassium content in untreated cells was 600 nmol/mg cell protein and was set at 100%. (D) ATP levels of the bacteria culture. Exponentially growing *E. coli* cells were resuspended to an O. D.<sub>650</sub> of 0.1 in a buffer containing 50 mM sodium Hepes (pH 7.0) and 5 mM glucose, and treated with nano-Ag (1 nM) or AgNO<sub>3</sub> (1  $\mu$ M) at room temperature. Aliquots of the bacteria culture were taken at timed intervals and the ATP levels were determined using a luciferase-luciferin enzymatic assay. The ATP level in untreated bacterial culture was 3 nmol/mg cell protein and was set at 100%.

mode of action of nano-Ag. It has previously been established that the translocation of envelope protein precursors across the inner (cytoplasmic) membrane, and their subsequent conversion to mature forms (i.e., cleavage of N-terminal signal sequence) require a functional plasma membrane having a transmembrane electrochemical potential, or membrane potential.<sup>34</sup> Agents that dissipate the membrane potential are known to induce an accumulation of envelope protein precursors in the cytoplasm.<sup>27,28,32,33</sup> In addition, the translocation of the envelope protein precursors also requires ATP.<sup>28,32,34,35</sup> We reasoned that the accumulation of these protein precursors in nano-Ag treated cells were perhaps mediated by the putative membrane destabilization and deenergization properties of nano-Ag. To assess such possibility, the effects of nano-Ag on bacterial membrane and ATP levels were investigated.

In *E. coli* cells, the outer membrane serves as a barrier to hydrophobic substances and macromolecules.<sup>36</sup> We first determined whether nano-Ag affected the integrity of the outer

membrane within *E. coli* cells. Destabilization of the outer membrane leads to an increased susceptibility to the bacteriolytic action of amphiphilic molecules such as detergents, which cannot penetrate an intact outer membrane.<sup>23,36</sup> Figure 4A shows that pretreatment of the *E. coli* cells with nano-Ag (1 nM, the MIC) sensitized the cells to rapid lysis by 0.1% SDS, as indicated by a decrease in the bacteria turbidity (O. D.<sub>650</sub>), whereas SDS alone had no effect. Similar results were obtained when cells were treated with AgNO<sub>3</sub> (1  $\mu$ M). Neither nano-Ag nor AgNO<sub>3</sub> affected the bacterial turbidity in the absence of SDS.

The effects of nano-Ag or AgNO<sub>3</sub> at their respective MICs on the cytoplasmic membrane potential of *E. coli* cells were examined using a fluorescence technique. diSC<sub>3</sub>(5) is a membrane potential probe whose fluorescence is quenched when it partitions to the electrically polarized cell membrane.<sup>24–26</sup> When the cytoplasmic membrane potential collapses, the probe is released back into the medium, resulting in fluorescence

recovery. As shown in Figure 4B, upon its addition to *E. coli* cells, the diSC<sub>3</sub>(5) fluorescence decreased gradually and stabilized after 10 min. Subsequent addition of nano-Ag (1 nM) or AgNO<sub>3</sub> (1  $\mu$ M) at its MIC resulted in a rapid recovery of fluorescence, indicative of a dissipation of the membrane potential. Valinomycin, a K<sup>+</sup> ionophore that equilibrates the K<sup>+</sup> concentration across the cytoplasmic membranes and dissipates the membrane potential, was used as a control for the membrane potential assays. Upon its addition, there was a rapid recovery of the diSC<sub>3</sub>(5) fluorescence similar to those mediated by the silver species.

As the membrane potential of *E. coli* is largely maintained by a high intracellular concentration of K<sup>+</sup> ions mediated by inward flux,<sup>46,47</sup> we further examined the effects of nano-Ag on cellular potassium contents. After a 5-min incubation, both nano-Ag and AgNO<sub>3</sub> added at their MIC elicited an almost complete loss of intracellular potassium (Figure 4C).

The ATP levels in *E. coli* cells after silver treatment were also determined. Figure 4D shows that both nano-Ag and AgNO<sub>3</sub>, when added at their MIC, depleted the ATP content of the bacterial cells in 5 min. There was no evidence of ATP leakage from the treated cells as revealed by measuring the ATP content of the medium.

## Discussion

We employed a proteomic approach (2-DE and MS identification) to help elucidate the mode of antibacterial action of nano-Ag, using *E. coli* as a model. Results from our proteomic analyses revealed that just a short exposure of *E. coli* cells to nano-Ag resulted in alterations in the expressions of a panel of envelope proteins (OmpA, OmpC, OmpF, OppA, MetQ) and heat shock proteins, (IbpA, IbpB and 30S ribosomal subunit S6) (Figure 2 and Table 1). Most of these proteins have been shown to be induced in a variety of stress conditions. The envelope proteins (OmpA, OmpC, OmpF, OppA, and MetQ) are integral outer membrane or periplasmic components guarding against the entry of foreign substances. Their expression is found to be sensitive to extreme osmolarity and pH.<sup>37–39</sup> The 30S ribosomal subunit S6, IbpA, and IbpB are heat shock proteins that have chaperone functions against stress induced protein denaturation.<sup>40–43</sup> In particular, the expression of IbpA and IbpB is stimulated during the overexpression of heterologous proteins that are associated inclusion bodies.<sup>41–43</sup> It remains to be investigated whether nano-Ag is detected analogously as intracellular foreign bodies. Supporting this argument, previous electron microscopic studies have provided some evidence for nano-Ag penetration into the *E. coli* cells.<sup>10</sup>

The most significant finding in our proteomic analysis is the identification of a number of envelope proteins (OmpA, OmpC, OmpF, OppA, and MetQ) whose expression was apparently induced by nano-Ag. These induced protein spots on the 2D gels have Mr and pI consistent with their full length forms (precursors); each of which contains an additional positively charged signal peptide of around 2 kDa (Table 2). This was confirmed by further immunoblot analysis on OmpA expression (Figure 3). Although the functional role of envelope proteins in the action of nano-Ag is not yet clear, the preferential accumulation of the precursor forms of a number of envelope proteins provide important hints to help identify the major mode of action of nano-Ag. It has been well established that the translocation of newly synthesized bacterial envelope membrane proteins is mediated by preprotein translocase and requires energy in the form of ATP and proton motive force;

the latter being established by a transmembrane pH gradient and transmembrane electrochemical potential (or membrane potential).<sup>28,32,34,35</sup> After the envelope protein precursors are properly inserted into the inner membrane of *E. coli* cells through a stepwise insertion mechanism, their positively charged N-terminal signal sequences are cleaved by membrane bound signal peptidases. Subsequently, the mature proteins are translocated across the membrane to the periplasm or outer membrane. In the absence of membrane potential or ATP, the precursor proteins are not incorporated into the inner membrane, and the signal sequences are not cleaved.<sup>27,28,31–35</sup> Consequently, the precursor proteins accumulate in the cytoplasm under these conditions. We reasoned that the accumulation of envelope proteins precursors in nano-Ag treated cells was due to the effects of that nano-Ag had on the bacterial membrane potential and/or ATP levels. In addition, we found that the proteome of nano-Ag treated cells contained induced proteins (proOmpC, proOmpF and IbpA) common to those found in the proteome of cells treated with an agent that uncoupled oxidative phosphorylation as well as an ATPase inhibitor.<sup>44</sup> Therefore, we further examined the effects of nano-Ag treatment on the properties of the bacterial membranes.

We found that treatment with nano-Ag destabilized the outer membrane (Figure 4A). This indicates that nano-Ag can disrupt the outer membrane barrier components such as lipopolysaccharide or porins,<sup>36</sup> culminating in the perturbation of the cytoplasmic membrane. Although the detailed mechanism by which nanoparticles with a diameter of 10 nm can penetrate and disrupt the membranes remains to be determined, electron microscopy and optical imaging results suggest that nano-Ag penetrate the outer and inner membranes of the treated Gram-negative bacteria, with some nanoparticles being found intracellularly.<sup>10,45</sup>

Nano-Ag elicited a rapid collapse of proton motive force (Figure 4B). This was also indicated by the observation that nano-Ag induced a massive loss of intracellular potassium (Figure 4C).<sup>46,47</sup> As expected, nano-Ag also decreased the cellular ATP levels (Figure 4D), apparently resulting from the collapse of membrane potential.<sup>48</sup> The rapid and complete depletion of ATP may be also indicative of a stimulation of hydrolysis of residual ATP. Previously, Ag<sup>+</sup> ions were reported to induce efflux of phosphate in *E. coli*<sup>15</sup> and stimulate rabbit mitochondrial ATP hydrolysis.<sup>49</sup>

It is conceivable that this dissipation of bacterial membrane potential and reduction of ATP levels by nano-Ag may culminate in loss of the cell viability. We have also demonstrated with proteomic and biochemical evidence that the pivotal antibacterial action of Ag<sup>+</sup> ions also involves membrane destabilization and deenergization in bacteria. This observation is consistent with previous studies on bacterial membrane vesicles, which revealed that Ag<sup>+</sup> ions induced a massive leakage of protons and a collapse of membrane potential.<sup>18</sup> The most significant difference between nano-Ag and Ag<sup>+</sup> ions is that their effective antibacterial concentrations lie within nanomolar and micromolar ranges, respectively. This suggests that nano-Ag mediate their antibacterial effects in a far more efficient physicochemical manner. However, further investigations are necessary to identify possible additional molecular targets for these silver species. In general, Ag<sup>+</sup> ions have high affinity for protein thiol groups,<sup>50</sup> and it has been suggested that thiol groups in key respiratory enzymes are possible sites for Ag<sup>+</sup> binding.<sup>14</sup> In this respect, we have also found that the antibacterial activities of nano-Ag, like those of Ag<sup>+</sup> ions, were

blocked by thiol containing agents (unpublished data). Alternatively, phospholipid portion of the bacterial membrane may also be the site of action for the silver species, as has previously been suggested for Ag<sup>+</sup> ions.<sup>18</sup>

## Conclusions

Through proteomic analyses, we have identified a possible mode of action of underlying the antibacterial action of nano-Ag. The proteomic signatures of nano-Ag treated *E. coli* cells are characterized by an accumulation of envelope protein precursors. This indicates that nano-Ag may target the bacterial membrane, leading to a dissipation of the proton motive force. The proteomic data are consistent with results from biochemical studies into the nano-Ag. In addition, nano-Ag and Ag<sup>+</sup> ions in the form of AgNO<sub>3</sub> appear to share a similar membrane-targeting mechanism of action. The effective concentrations of nano-Ag and Ag<sup>+</sup> ions are at nanomolar and micromolar levels, respectively. Nano-Ag appear to be significantly more efficient than Ag<sup>+</sup> ions in mediating their antimicrobial activities.

**Abbreviations.** nano-Ag, silver nanoparticles; SPR, surface plasmon resonance; TEM, transmission electron microscopy; HRTEM, high-resolution transmission electron microscopy; ICP-MS, inductive coupled plasma-mass spectrometry; 2-DE, two-dimensional electrophoresis; IEF, isoelectric focusing; CHAPS, 3[(3-cholamidopropyl) dimethylammonio]-1-propane-sulfonate; MALDI-TOF MS, matrix assisted laser desorption/ionization time-of-flight mass spectrometry; SDS, sodium dodecyl sulfate; PAGE, polyacrylamide gel electrophoresis; diSC<sub>3</sub>(5), dipropylthiadiazocarbocyanine iodide; FAES, flame atomic emission spectroscopy; MIC, minimum inhibitory concentration; OmpA, OmpC, and OmpF, outer membrane proteins A, C, and F, respectively; OppA, periplasmic oligopeptide binding protein A; MetQ, D-methionine binding lipoprotein; IbpA and B, inclusion body binding proteins A and B.

**Acknowledgment.** We thank Prof. Arnold Driessen for providing OmpA antibodies and the *E. coli* Genetic Stock Centre for providing the bacteria. We are grateful to Dr. Rory Watt for comments on the manuscript. This work is supported by the Area of Excellence Scheme (AoE/P-10/01) established under the University Grants Committee of the Hong Kong Special Administrative Region, People's Republic of China, the Research Support Programs and Focused Research Themes of the University Research Committee of the University of Hong Kong.

**Supporting Information Available:** MS data for the identified *E. coli* proteins whose expressions were stimulated by nano-Ag. This material is available free of charge via the Internet at <http://pubs.acs.org>.

## References

- (1) Russell, A. D.; Hugo, W. B. Antimicrobial activity and action of silver. *Prog. Med. Chem.* **1994**, *31*, 351–370.
- (2) Silver, S. Bacterial silver resistance: molecular biology and uses and misuses of silver compounds. *FEMS Microbiol. Rev.* **2003**, *27*, 341–353.
- (3) Klasen, H. J. A historical review of the use of silver in the treatment of burns. II. Renewed interest for silver. *Burns* **2000**, *26*, 131–138.
- (4) Fan, F.-R. F.; Bard, A. J. Chemical, electrochemical, gravimetric, and microscopic studies on antimicrobial silver films. *J. Phys. Chem. B* **2002**, *106*, 279–287.
- (5) Balogh, L.; Swanson, D. R.; Tomalia, D.; Hagnauer, G. L.; McManus, A. T. Dendrimer-silver complexes and nanocomposites as antimicrobial agents. *Nano Lett.* **2001**, *1*, 18–21.

- (6) Friedenthal, H. *Biochem. Z.* **1919**, *94*, 47.
- (7) Baker, C.; Pradhan, A.; Pakstis, L.; Pochan, D. J.; Shah, S. I. Synthesis and antibacterial properties of silver nanoparticles. *J. Nanosci. Nanotechnol.* **2005**, *5*, 244–249.
- (8) Aymonier, C.; Schlotterbeck, U.; Antonietti, L.; Zacharias, P.; Thomann, R.; Tiller, J. C.; Mecking, S. Hybrids of silver nanoparticles with amphiphilic hyperbranched macromolecules exhibiting antimicrobial properties. *Chem. Commun.* **2002**, 3018–3019.
- (9) Melaiye, A.; Sun, Z.; Hindi, K.; Milsted, A.; Ely, D.; Reneker, D. H.; Tessier, C. A.; Youngs, W. J. Silver(I)-imidazole cyclophane gem-diol complexes encapsulated by electrospun tefophilic nanofibers: formation of nanosilver particles and antimicrobial activity. *J. Am. Chem. Soc.* **2005**, *127*, 2285–2291.
- (10) Sondi, I.; Salopek-Sondi, B. Silver nanoparticles as antimicrobial agent: a case study on *E. coli* as a model for Gram-negative bacteria. *J. Colloid Interface Sci.* **2004**, *275*, 177–182.
- (11) Alt, V.; Bechert, T.; Steinrucke, P.; Wagener, M.; Seidel, P.; Dingeldein, E.; Domann, E.; Schnetzler, R. An in vitro assessment of the antibacterial properties and cytotoxicity of nanoparticulate silver bone cement. *Biomaterials* **2004**, *25*, 4383–4391.
- (12) Wright, J. B.; Lam, K.; Buret, A. G.; Olson, M. E.; Burrell, R. E. Early healing events in a porcine model of contaminated wounds: effects of nanocrystalline silver on matrix metalloproteinases, cell apoptosis, and healing. *Wound Repair Regen.* **2002**, *10*, 141–151.
- (13) Sun, R. W.; Chen, R.; Chung, N. P.; Ho, C. M.; Lin, C. L.; Che, C. M. Silver nanoparticles fabricated in Hepes buffer exhibit cytoprotective activities toward HIV-1 infected cells. *Chem. Comm.* **2005**, 5059–5061.
- (14) Bard, A. J.; Holt, K. B. Interaction of Silver(I) Ions with the Respiratory Chain of *Escherichia coli*: An Electrochemical and Scanning Electrochemical Microscopy Study of the Antimicrobial Mechanism of Micromolar Ag<sup>+</sup>. *Biochemistry* **2005**, *44*, 13214–13223.
- (15) Schreurs, W. J.; Rosenberg, H. Effect of silver ions on transport and retention of phosphate by *Escherichia coli*. *J. Bacteriol.* **1982**, *152*, 7–13.
- (16) Bragg, P. D.; Rainnie, D. J. The effect of silver ions on the respiratory chain of *Escherichia coli*. *Can. J. Microbiol.* **1974**, *228*, 883–889.
- (17) Semeykina, A. L.; Skulachev, V. P. Submicromolar Ag<sup>+</sup> increases passive Na<sup>+</sup> permeability and inhibits the respiration-supported formation of Na<sup>+</sup> gradient in *Bacillus* FTU vesicles. *FEBS Lett.* **1990**, *269*, 69–72.
- (18) Dibrov, P.; Dzioba, J.; Gosink, K. K.; Hase, C. C. Chemiosmotic mechanism of antimicrobial activity of Ag<sup>+</sup> in *Vibrio cholerae*. *Antimicrob. Agents Chemother.* **2002**, *46*, 2668–2670.
- (19) Feng, Q. L.; Wu, J. L.; Chen, G. Q.; Cui, F. Z.; Kim, T. N.; Kim, J. O. A mechanistic study of the antibacterial effect of silver ions on *Escherichia coli* and *Staphylococcus aureus*. *J. Biomed. Mater. Res.* **2000**, *52*, 662–668.
- (20) Ghandour, W.; Hubbard, J. A.; Deistung, J.; Hughes, M. N.; Poole, R. K. The uptake of silver ions by *Escherichia coli* K12: Toxic effects and interaction with copper ions. *Appl. Microbiol. Biotechnol.* **1994**, *28*, 559–565.
- (21) Jin, R.; Cao, Y.; Mirkin, C. A.; Kelly, K. L.; Schatz, G. C.; Zheng, J. G. Photoinduced conversion of silver nanospheres to nanoprisms. *Science* **2001**, *294*, 1901–1903.
- (22) Gan, X.; Liu, T.; Zhong, J.; Liu, X.; Li, G. Effect of silver nanoparticles on the electron-transfer reactivity and the catalytic activity of myoglobin. *Chembiochem.* **2004**, *5*, 1686–1691.
- (23) Helander, I. M.; Alakomi, H. L.; Latva-Kala, K.; Koski, P. Polyethyleneimine is an effective permeabilizer of gram-negative bacteria. *Microbiology* **1997**, *143*, 3193–3199.
- (24) Letellier, L.; Shechter, E. Cyanine dye as monitor of membrane potentials in *Escherichia coli* cells and membrane vesicles. *Eur. J. Biochem.* **1979**, *102*, 441–447.
- (25) Wu, M.; Maier, E.; Benz, R.; Hancock, R. E. Mechanism of interaction of different classes of cationic antimicrobial peptides with planar bilayers and with the cytoplasmic membrane of *Escherichia coli*. *Biochemistry* **1999**, *38*, 7235–7242.
- (26) Herranz, C.; Cintas, L. M.; Hernandez, P. E.; Moll, G. N.; Driessen, A. J. M. Enterocin P causes potassium ion efflux from *Enterococcus faecium* T136 cells. *Antimicrob. Agents Chemother.* **2001**, *45*, 901–904.
- (27) Beher, M. G.; Schnaitman, C. A. Regulation of the OmpA outer membrane protein of *Escherichia coli*. *J. Bacteriol.* **1981**, *147*, 972–985.
- (28) Zimmermann, R.; Wickner, W. Energetics and intermediates of the assembly of Protein OmpA into the outer membrane of *Escherichia coli*. *J. Biol. Chem.* **1983**, *258*, 3920–3925.

- (29) Rodionova, N. A.; Tatulian, S. A.; Surrey, T.; Jahnig, F.; Tamm, L. K. Characterization of two membrane-bound forms of OmpA. *Biochemistry* **1995**, *34*, 1921–1929.
- (30) Wang, Y. The function of OmpA in *Escherichia coli*. *Biochem. Biophys. Res. Commun.* **2002**, *292*, 396–401.
- (31) Crowlesmith, I.; Gamon, K. Rate of translation and kinetics of processing of newly synthesized molecules of two major outer-membrane proteins, the OmpA and OmpF proteins, of *Escherichia coli* K12. *Eur. J. Biochem.* **1982**, *124*, 577–583.
- (32) Driessen, A. J.; Wickner, W. Proton transfer is rate-limiting for translocation of precursor proteins by the *Escherichia coli* translocase. *Proc. Natl. Acad. Sci. U.S.A.* **1991**, *88*, 2471–2475.
- (33) Pages, J. M.; Lazdunski, C. Membrane potential ( $\Delta\psi$ ) depolarizing agents inhibit maturation. *FEBS Lett.* **1982**, *149*, 51–54.
- (34) Randall, L. L. Function of protonmotive force in translocation of protein across membranes. *Methods Enzymol.* **1986**, *125*, 129–138.
- (35) Driessen, A. J. Precursor protein translocation by the *Escherichia coli* translocase is directed by the protonmotive force. *EMBO J.* **1992**, *11*, 847–853.
- (36) Vaara, M. Agents that increase the permeability of the outer membrane. *Microbiol. Rev.* **1992**, *56*, 395–411.
- (37) Stancik, L. M.; Stancik, D. M.; Schmidt, B.; Barnhart, D. M.; Yoncheva, Y. N.; Slonczewski, J. L. pH-dependent expression of periplasmic proteins and amino acid catabolism in *Escherichia coli*. *J. Bacteriol.* **2002**, *184*, 4246–4258.
- (38) Sato, M.; Machida, K.; Arikado, E.; Saito, H.; Kakegawa, T.; Kobayashi, H. Expression of outer membrane proteins in *Escherichia coli* growing at acid pH. *Appl. Environ. Microbiol.* **2000**, *66*, 943–947.
- (39) Heyde, M.; Coll, J. L.; Portalier, R. Identification of *Escherichia coli* genes whose expression increases as a function of external pH. *Mol. Gen. Genet.* **1991**, *229*, 197–205.
- (40) Otani, M.; Tabata, J.; Ueki, T.; Sano, K.; Inouye, S. Heat-shock-induced proteins from *Myxococcus xanthus*. *J. Bacteriol.* **2001**, *183*, 6282–6287.
- (41) Jakob, U.; Gaestel, M.; Engel, K.; Buchner, J. Small heat shock proteins are molecular chaperones. *J. Biol. Chem.* **1993**, *268*, 1517–1520.
- (42) Kitagawa, M.; Matsumura, Y.; Tsuchido, T. Small heat shock proteins, IbpA and IbpB, are involved in resistances to heat and superoxide stresses in *Escherichia coli*. *FEMS Microbiol. Lett.* **2000**, *184*, 165–171.
- (43) Allen, S. P.; Polazzi, J. O.; Gierse, J. K.; Easton, A. M. Two novel heat shock genes encoding proteins produced in response to heterologous protein expression in *Escherichia coli*. *J. Bacteriol.* **1992**, *174*, 6938–6947.
- (44) VanBogelen, R. A.; Schiller, E. E.; Thomas, J. D.; Neidhardt, F. C. Diagnosis of cellular states of microbial organisms using proteomics. *Electrophoresis* **1999**, *20*, 2149–2159.
- (45) Xu, X. H.; Brownlow, W. J.; Kyriacou, S. V.; Wan, Q.; Viola, J. J. Real-time probing of membrane transport in living microbial cells using single nanoparticle optics and living cell imaging. *Biochemistry* **2004**, *43*, 10400–10413.
- (46) Epstein, W. The roles and regulation of potassium in bacteria. *Prog. Nucleic Acid Res. Mol. Biol.* **2003**, *75*, 293–320.
- (47) Lambert, P. A.; Hammond, S. M. Potassium fluxes, first indications of membrane damage in microorganisms. *Biochem. Biophys. Res. Commun.* **1973**, *54*, 796–799.
- (48) Dimroth, P.; Kaim, G.; Matthey, U. Crucial role of the membrane potential for ATP synthesis by F(1)F(o) ATP synthases. *J. Exp. Biol.* **2000**, *203*, 51–59.
- (49) Chappell, J. B.; Greville, G. D. Effect of silver ions on mitochondrial adenosine triphosphatase. *Nature* **2005**, *174*, 930–931.
- (50) Liao, S. Y.; Read, D. C.; Pugh, W. J.; Furr, J. R.; Russell, A. D. Interaction of silver nitrate with readily identifiable groups: relationship to the antibacterial action of silver ions. *Lett. Appl. Microbiol.* **1997**, *25*, 279–283.

PR0504079